J|A|C|S
ARTICLES
Published on Web 02/01/2002

Catalytic Mechanism of Heme Oxygenase through EPR and ENDOR of Cryoreduced Oxy-Heme Oxygenase and Its Asp 140 Mutants

Roman Davydov,[†] Viktoria Kofman,[†] Hiroshi Fujii,[‡] Tadashi Yoshida,[§] Masao Ikeda-Saito,[||] and Brian M. Hoffman*[,†]

Contribution from the Department of Chemistry, Northwestern University, Evanston, Illinois 60208, Institute for Molecular Science, Mydaiji, Okazaki 444-8585, Japan, Department of Biochemistry, Yamagata University School of Medicine, Yamagata 990-23, Japan, Department of Physiology and Biophysics, Case Western University School of Medicine, Cleveland, Ohio 44106-4970, and Institute of Multidisciplinary Research for Advanced Materials, Tohoku University, Sendai 980-8577, Japan

Received September 25, 2001

Abstract: Heme oxygenase (HO) catalyzes the O_2- and NADPH-cytochrome P450 reductase-dependent conversion of heme to biliverdin, Fe, and CO through a process in which the heme participates both as a prosthetic group and as a substrate. In the present study, we have generated a detailed reaction cycle for the first monooxygenation step of HO catalysis, conversion of the heme to α-*meso*-hydroxyheme. We employed EPR (using both $^{16}O_2$ and $^{17}O_2$) and ^{1}H, ^{14}N ENDOR spectroscopies to characterize the intermediates generated by 77 K radiolytic cryoreduction and subsequent annealing of wild-type oxy-HO and D140A, F mutants. One-electron cryoreduction of oxy-HO yields a hydroperoxoferri-HO with **g**-tensor, **g** = [2.37, 2.187, 1.924]. Annealing of this species to 200 K is accompanied by spectroscopic changes that include the appearance of a new ^{1}H ENDOR signal, reflecting rearrangements in the active site. Kinetic measurements at 214 K reveal that the annealed hydroperoxoferri-HO species, denoted **R**, generates the ferri-α-*meso*-hydroxyheme product in a first-order reaction. Disruption of the H-bonding network within the distal pocket of HO by the alanine and phenylalanine mutations of residue D140 prevents product formation. The hydroperoxoferri-HO (D140A) instead undergoes heterolytic cleavage of the O−O bond, ultimately yielding an EPR-silent compound II-like species that does not form product. These results, which agree with earlier suggestions, establish that hydroperoxoferri-HO is indeed the reactive species, directly forming the α-*meso*-hydroxyheme product by attack of the distal OH of the hydroperoxo moiety at the heme α-carbon.

Heme oxygenase (HO) catalyzes the O_2- and NADPH-cytochrome P450 reductase-dependent conversion of heme to biliverdin, Fe, and CO, Scheme 1, through a process in which the heme participates both as a prosthetic group and as a substrate.[1−3] In the HO catalytic cycle, the enzyme first forms a heme−protein complex in which the heme-iron coordinates to a neutral imidazole of histidine, as in myoglobin (Mb) and hemoglobin (Hb).[4,5] It was proposed[1,2] that the first monooxygenation step of HO catalysis is the conversion of the heme to α-*meso*-hydroxyheme. In this mechanism, an electron provided by NADPH-cytochrome P450 reductase first reduces the ferric heme to the ferrous state, and a molecule of dioxygen binds to form a metastable O_2-bound complex, which is reduced by a second electron to generate hydroperoxy-ferri-HO. It was further thought that the hydroperoxy-ferri-HO is the reactive hydroxylating species,[2] rather than a high-valent ferryl active intermediate as in the case of cytochrome P450cam.[6,7] However, neither the putative hydroperoxoferri-HO intermediate nor the α-*meso*-hydroxyheme product had been detected during physiological HO catalysis until our recent EPR and ENDOR study of oxy-ferrous HO cryoreduced at 77 K.[8] This study established that the hydroperoxy-ferri-HO indeed is formed upon the cryoreduction of oxy-HO, that its decay leads to the formation of α-*meso*-hydroxyheme, and that this can occur in situ at cryogenic temperatures.

One-electron radiolytic cryoreduction[9,10] of diamagnetic oxy-hemoproteins in frozen solution at 77 K[7,11−16] creates a

[†] Northwestern University.
[‡] Institute for Molecular Science.
[§] Yamagata University School of Medicine.
[||] Case Western University School of Medicine and Tohoku University.

(1) Wilks, A.; Ortiz de Montellano, P. R. *J. Biol. Chem.* **1993**, *268*, 22357−22362.
(2) Ortiz de Montellano, P. R. *Acc. Chem. Res.* **1998**, *31*, 543−549.
(3) Migita, C. T.; Matera, K. M.; Ikeda-Saito, M.; Olson, J. S.; Fujii, H.; Yoshimura, T.; Zhou, H.; Yoshida, T. *J. Biol. Chem.* **1998**, *273*, 945−949.
(4) Yoshida, T.; Kikuchi, G. *J. Biol. Chem.* **1978**, *253*, 4224−4229.
(5) Yoshida, T.; Kikuchi, G. *J. Biol. Chem.* **1979**, *254*, 4487−4491.
(6) Ortiz de Montellano, P. R.; Correia, M. A. *Cytochrome P450*; Plenum Press: New York, 1995; Vol. 2.
(7) Davydov, R.; Makris, T. M.; Kofman, V.; Werst, D. W.; Sligar, S. G.; Hoffman, B. M. *J. Am. Chem. Soc.* **2001**, *123*, 1403−1415.
(8) Davydov, R. M.; Yoshida, T.; Ikeda-Saito, M.; Hoffman, B. M. *J. Am. Chem. Soc.* **1999**, *121*, 10656−10657.
(9) Davydov, R.; Kuprin, S.; Graslund, A.; Ehrenberg, A. *J. Am. Chem. Soc.* **1994**, *116*, 11120−11128.

10.1021/ja0122391 CCC: $22.00

Scheme 1

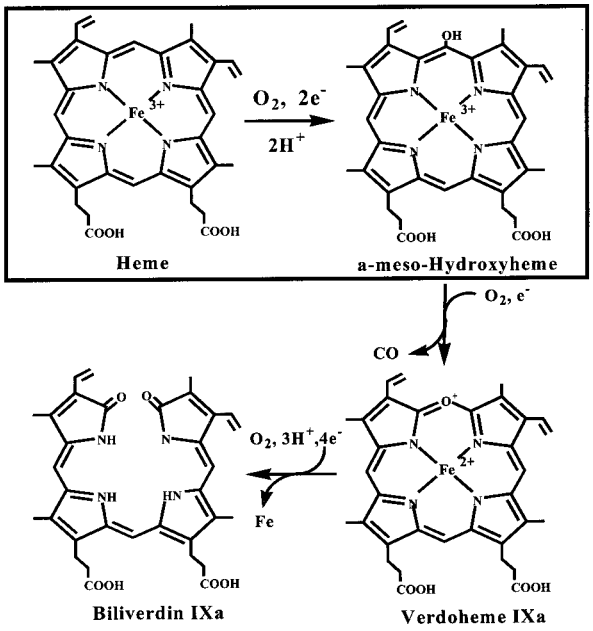

paramagnetic species trapped in the environment of the precursor oxy-heme; annealing to higher temperature permits the reduced heme pocket to relax to its equilibrium conformational state. Subsequent annealing stages permit an enzyme, such as P450cam or HO, to step-by-step traverse its catalytic cycle, through product formation, with the combination of EPR and ENDOR measurements providing an optimal means of characterizing the individual stages in catalysis.[7,8,16] Through such measurements we concluded that reduction of oxy-HO at 77 K directly generates the hydroperoxoferri-HO (denoted here, **P**),[8] and likewise for cytochrome P450cam and its T252A mutant.[7,16] Thus, even at this temperature the first proton of catalysis in a dioxygen-activating enzyme can be delivered to the heme-bound dioxygen upon reduction of the oxy-ferroheme. This is in contrast to the case of proteins such as Hb and Mb,[11−14] which are designed for carrying dioxygen rather than activating it. Reduction of oxy-Mb and -Hb at 77 K generates a peroxoferric intermediate, and annealing at $T \geq 180$ K is needed to form the hydroperoxo species.[11,13]

In the present study, we have generated a detailed reaction cycle for the first monooxygenation step of HO catalysis through use of EPR (using both $^{16}O_2$ and $^{17}O_2$) and ^{1}H, ^{14}N ENDOR spectroscopies to characterize the intermediates generated by 77 K radiolytic cryoreduction and subsequent annealing of oxy-HO. We have examined both WT enzyme and mutants at Asp140. This residue, which is located in the heme pocket, Figure 1, plays a central role in a distal-pocket H-bonding network, and its mutants exhibit dramatic alterations in catalytic function.[17,18] Such measurements recently confirmed that the

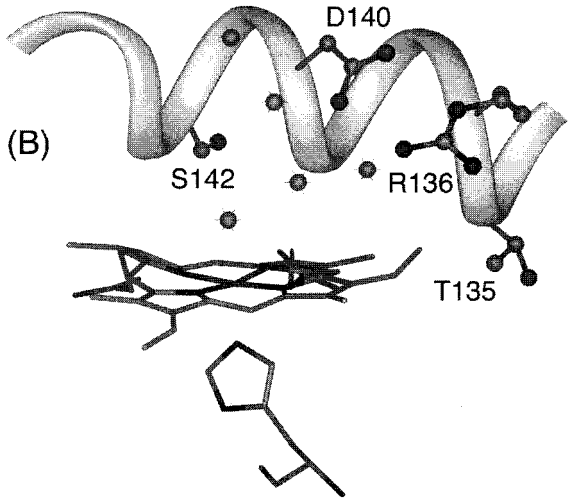

Figure 1. Structure of the HO heme pocket.[17]

active hydroxylation intermediate in P450cam is a high-valent ferryl active intermediate.[6,7] The present study instead establishes that hydroperoxoferri-HO is indeed the reactive hydroxylating species, which directly forms the α-*meso*-hydroxyheme product by attack of the distal OH of the hydroperoxo moiety at the heme α-carbon.[2] The hydroperoxoferri-HO (D140A) instead undergoes heterolytic cleavage of the O−O bond, presumably first forming a compound I, while ultimately yielding an EPR-silent compound II-like species that does not form product.

Materials and Methods

The wild type (WT) and D140A and F mutants of truncated water-soluble forms of recombinant rat HO-1 (denoted HO) were expressed, purified, and reconstituted with hemin according to published procedures.[18] The oxy-HO (WT) was prepared by dithionite reduction of anaerobic solutions of ferri-HO followed by aerobic chromatography on a G25 column equilibrated with 0.1 M KP_i (pH 7) at 4 °C. The oxy-HO (D140X), X = A, F, complexes were prepared in two different ways. In the first, the anaerobic solution of the oxidized mutant in 0.1 M KP_i−ethylene glycol (1:1 v/v), pH 7, was reduced by a 2-fold molar excess of dithionite at 20 °C followed by bubbling the solution with O_2 at −20 °C for 3 min. In the second way the mutant solution in 0.1 M KP_i (pH 7) containing 15% glycerol was bubbled with CO for 1 min and then was reduced by a 2-fold molar excess of dithionite. The solution was then bubbled with O_2 for 2 min at −5 °C. The experimental results were independent of the way of the oxycomplex preparation. The samples typically contained 1−1.5 mM protein, 0.1 M KP_i (pH 7.0), and 15% v/v glycerol. As desired, samples were exchanged four times in D_2O buffers. All samples were stored in quartz EPR tubes at 77 K. The oxy-samples were reduced at 77 K by γ-irradiation with a ^{60}Co source (Gammacell 220) to a dose ∼3 Mrad as described elsewhere[10] and were then kept at 77 K.

As desired, the cryoreduced samples were annealed at temperatures above 77 K by transferring a sample from liquid nitrogen to a bath at fixed temperature for 1 min unless specified otherwise, after which the sample was transferred back to liquid nitrogen. Examination of a thermocouple frozen in a Q-band tube (2.5 mm o.d.) showed that an approximate equilibrium with the bath occurred in ∼15−20 s. Thus, for example, a reported 1 min of annealing at temperature *T* corresponds to ∼40−45 s at *T*. The clock time and the time at temperature obviously

(10) Davydov, R.; Valentine, A. M.; Komar-Panicucci, S.; Hoffman, B. M.; Lippard, S. J. *Biochemistry* **1999**, *38*, 4188−4197.
(11) Symons, M. C. R.; Petersen, R. L. *Proc. R. Soc. London, Ser. B* **1978**, *201*, 285−300.
(12) Davydov, R. M. *Biofizika* **1980**, *25*, 203−207.
(13) Kappl, R.; Höhn-Berlage, M.; Hüttermann, J.; Bartlett, N.; Symons, M. C. R. *Biochim. Biophys. Acta* **1985**, *827*, 327−343.
(14) Leibl, W.; Nitschke, W.; Hüttermann, J. *Biochim. Biophys. Acta* **1986**, *870*, 20−30.
(15) Davydov, R.; Kappl, R.; Hutterman, R.; Peterson, J. *FEBS Lett.* **1991**, *295*, 113−115.
(16) Davydov, R.; Macdonald, I. D. G.; Makris, T. M.; Sligar, S. G.; Hoffman, B. M. *J. Am. Chem. Soc.* **1999**, *121*, 10654−10655.
(17) Lightning, L. K.; Huang, H.-w.; Möane-Loccoz, P.; Loehr, T. M.; Schuller, D. J.; Poulos, T. L.; Ortiz de Montellano, P. R. *J. Biol. Chem.* **2001**, *276*, 10612−10619.
(18) Fujii, H.; Zhang, X.; Tomita, T.; Ikeda-Saito, M.; Yoshida, T. *J. Am. Chem. Soc.* **2001**, *123*, 6475−6484.

agree more closely, the longer an annealing step is carried out. For consistency, however, we quote clock times for annealing, regardless. Each cryoreduction and annealing process discussed here was repeated several times with results that are wholly compatible, but that vary slightly in the apparent degree of a particular conversion at a particular bath temperature as the result of the imprecision associated with the short annealing periods.

X-band EPR spectra were recorded on a modified Varian E-4 spectrometer at 77 K. Q-band (35 GHz) EPR and ENDOR spectra were recorded on a modified Varian E-110 spectrometer equipped with a helium immersion dewar. These spectra, which were obtained in dispersion mode using 100 kHz field modulation under "rapid passage" conditions,[19−21] have the appearance of absorption spectra; derivative presentations were generated digitally using LabCalc. For ENDOR, in some instances, the radio frequency (RF) bandwidth was broadened to 60−100 kHz to improve the signal-to-noise ratio.[22] EPR spectra of cryoreduced samples exhibit strong signals from free radicals created by the irradiation; this region is deleted from the spectra shown. The EPR signals of the cryoreduced oxy-HO were quantitated using a 1 mM solution of $Cu(ClO_4)_2$ as a standard.

For a single orientation of a paramagnetic center, the first-order ENDOR spectrum of a nucleus with $I = {}^1/_2$ in a single paramagnetic center consists of a doublet with frequencies given by[23]

$$\nu_{\pm} = |\nu_N \pm A/2| \quad (1)$$

Here, ν_N is the nuclear Larmor frequency, and A is the orientation-dependent hyperfine coupling constant of the coupled nucleus. The doublet is centered at the Larmor frequency and separated by A when $\nu_N > |A/2|$, as is the case for ^{1}H spectra presented here. For ^{14}N ($I = 1$), a single orientation gives a four-line pattern

$$\nu_{\pm}(\pm) = |\nu_N \pm A/2 \pm 3P/2| \quad (1a)$$

in which both the ν_+ and the ν_- branches described by eq 1 are further split into two lines by the quadrupole splitting, $3P$. For heme pyrrole ^{14}N studied here, only the $\nu_+(\pm)$ branch is readily observed in spectra collected at 35 GHz. The full hyperfine and quadrupole tensors of a coupled nucleus can be obtained by analyzing a 2-D field-frequency set of orientation-selective ENDOR spectra collected across the EPR envelope, as described elsewhere.[24,25]

Results

EPR Spectroscopy of Cryoreduced Oxy-HO. Primary Product of 77 K Cryoreduction. Figure 2, upper, presents a 2 K Q-band EPR spectrum of a sample of HO-O_2 that has undergone 77 K cryoreduction. The low-field region (not shown) exhibits the $g_\perp = 5.75$ feature of residual high-spin aquoferri-HO.[26] The higher-field region presented is dominated by a rhombic, low-spin ferriheme signal which was not present prior to reduction, along with signals near $g = 2$ from radicals caused by the γ-irradiation. Careful examination of the signal shows that it comes from a majority species, denoted **P**, with **g** = [2.37, 2.187, 1.924], plus weak features come from a minority form (denoted **P1**) that flank the g_2 feature of **P**. This spectrum of **P**, which corresponds to roughly 40% of the oxy-HO initially present in the sample, is qualitatively similar to that of a variety of hydroperoxoferri-proteins, including Mb and Hb,[11−14] P450cam,[7] and alkyl-peroxoferriheme model compounds,[27] and we ascribed it previously to hydroperoxoferri-HO. This assignment is confirmed below.

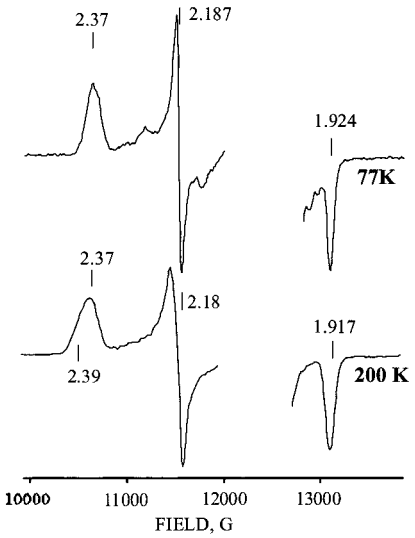

Figure 2. EPR spectra of oxy-HO cryoreduced at 77 K (upper) and annealed at 200 K for 1 min (lower). Free radical signals around $g = 2$ are omitted for clarity. Conditions: 35.256 GHz, $T = 2$ K, 100 Khz field modulation, modulation amplitude 1 G, microwave power 30 db.

Annealing Measurements: 77−200 K. Cryoreduced samples were progressively annealed in numerous small steps, as described in Materials and Methods, and were examined by EPR after each step.

The amplitude and shape of the residual high-spin ferriheme signal are unchanged by annealing to 200 K. During this annealing process, the amount of the low-spin hydroperoxoferri-HO likewise appears to remain the same. However, the annealing slightly alters the EPR spectrum of the low-spin hydroperoxoferri-HO. As shown in Figure 2, lower, in the EPR spectrum of the sample annealed at 200 K, the g_1 feature remains at $g_1 = 2.37$ but shows asymmetric broadening to lower field; the g_2 feature shifts from 2.187 to 2.180 and gets slightly asymmetric, while the g_3 component broadens and shifts from 1.924 to 1.917. Although these changes are small, the shifts are reliably detected in the 35 GHz spectra and are taken to indicate that during this annealing **P** relaxes to a slightly altered hyroperoxoferri-HO species, denoted **R**, which has slightly different interactions with the distal pocket; the full annealing protocol shows that the relaxation process begins with a 1 min warming to ∼140 K and is essentially complete by ∼180 K. The asymmetry of the g_1 and g_2 features in the EPR spectrum of the annealed hydroperoxo intermediate indicates the presence of a minority species, denoted **R1**, with slightly larger g anisotropy: **g** ≈ [2.393, 2.188, 1.917].

Further Characterization of P/P1 and R/R1 Intermediates. The **g**-tensor of the primary species **P/P1** and of the relaxed state **R/R1** deviates somewhat from those of the analogous

(19) Werst, M. M.; Davoust, C. E.; Hoffman, B. M. *J. Am. Chem. Soc.* **1991**, *113*, 1533−1538.
(20) Mailer, C.; Taylor, C. P. S. *Biochim. Biophys. Acta* **1973**, *322*, 195−203.
(21) Feher, G. *Phys. Rev.* **1959**, *114*, 1219−1244.
(22) Hoffman, B. M.; DeRose, V. J.; Ong, J. L.; Davoust, C. E. *J. Magn. Reson.* **1994**, *110*, 52−57.
(23) Abragam, A.; Bleaney, B. *Electron Paramagnetic Resonance of Transition Metal Ions*, 2nd ed.; Clarendon Press: Oxford, 1970.
(24) Hoffman, B. M. *Acc. Chem. Res.* **1991**, *24*, 164−170.
(25) Hoffman, B. M.; DeRose, V. J.; Doan, P. E.; Gurbiel, R. J.; Houseman, A. L. P.; Telser, J. In *Biological Magnetic Resonance*; Berliner, L. J., Reuben, J., Eds.; Plenum Press: New York and London, 1993; Vol. 13, pp 151−218.
(26) Matera, K. M.; Takahashi, S.; Fujii, H.; Zhou, H.; Ishikawa, K.; Yoshimura, T.; Rousseau, D. L.; Yoshida, T.; Ikeda-Saito, M. *J. Biol. Chem.* **1996**, *271*, 6618−6624.
(27) Tajima, K.; Edo, T.; Ishizu, K.; Imaoka, S.; Funae, Y.; Oka, S.; Sakurai, H. *Biochem. Biophys. Res. Commun.* **1993**, *191*, 157−164.

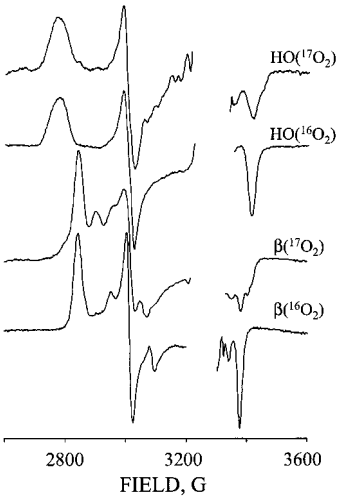

Figure 3. X-band EPR spectra of HO-$^{17}O_2$, HO-$^{16}O_2$, Hbβ-$^{17}O_2$, and Hbβ-$^{16}O_2$ cryoreduced at 77 K and annealed at 190 K for 1 min. Free radical signals are omitted for clarity. Conditions: $T = 77$ K, modulation amplitude 1.25 G, MW power 5 mW, MW frequency 9.223 GHz.

species in other heme proteins. In particular, $g_1 = 2.37$ for the hydroperoxoferri-HO is noticeably greater than that of known hydroperoxoferric complexes, such as that of the β chains of Hb, where $\mathbf{g} = [2.31, 2.18, 1.94]$ (Figure 3). To corroborate the assignment in HO to a hydroperoxoferriheme, we examined the "hydroperoxo" moiety of these species through use of $^{17}O_2$ and by proton ENDOR, and we examined the heme portion by ^{14}N ENDOR of the pyrroles.

$^{17}O_2$-HO. Our assignment of **P** and **R** as hyroperoxoferriheme states is supported by comparison of measurements on cryoreduced oxy($^{17}O_2$)-HO, with parallel measurements on oxy($^{17}O_2$)-β-Hb. Focusing on the reactive hydroperoxo(^{17}O)-ferri-HO species **R** seen after annealing at ~200 K (see below), Figure 3 shows that the ^{17}O labeling of **R** does not yield resolved hyperfine couplings, but rather produces a broadened g_3 feature, with lesser broadening at the other g features. Simulations where it is assumed that the proximal ^{17}O (isotopic abundance, 83%) of the $[OOH]^-$ ligand is hyperfine-coupled indicate that $A(g_3) \approx 5-7$ G.

This contrasts with the ^{17}O coupling in the primary product in cryoreduction of nonenzymatic hemoproteins such as oxy-Hb/Mb, which is assigned as a "H-bonded-peroxoferriheme".[11,13,14] This species shows resolvable splittings at g_3 from the $^{17}O_2$ moiety, $A(g_3) \approx 25$ G, arising from spin delocalization from Fe to the π^* orbitals on the peroxo ligand.[11,13] Upon annealing this species, it converts to the hydroperoxoferric form. Previous work with low-enrichment $^{17}O_2$ did not detect either resolved splitting or broadening from ^{17}O in the hydroperoxo complex, compatible with reduced delocalization in this state. We reexamined this state with the higher-enrichment $^{17}O_2$ (83%) by collecting EPR spectra of hydroperoxoferri-β-Hb prepared by cryoreducing oxy($^{17}O_2$)-β-Hb and annealing to 200 K.[8] As shown in Figure 3, the EPR spectrum of this hydroperoxo(^{17}O)-ferri-β-Hb in fact shows the small ^{17}O broadening seen with HO, and simulations of the two spectra both give an ^{17}O coupling of $A_3 \approx 5-7$ G, confirming that the two proteins contain hydroperoxo ligands with comparable bonding to the ferric ion.

^{14}N ENDOR Studies of P and R Intermediates. ENDOR examination of the pyrrole ^{14}N provides a means to characterize

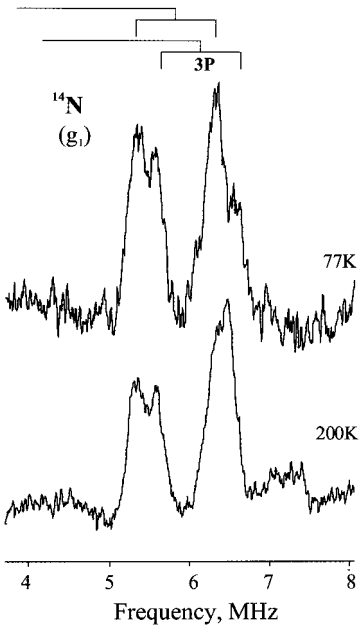

Figure 4. ^{14}N ENDOR spectra taken at $g_1 = 2.37$ for oxy-HO radiolytically reduced at 77 K, intermediate **P**; after annealing at 200 K for 1 min, intermediate **R**; and after 2 min at 214 K. "Brackets" indicate the $\nu_+(\pm)$ branches for two nearly equivalent ^{14}N, with the quadrupole splittings (3*P*) indicated. For parameters, see text. Conditions: $T = 2$ K, field modulation 100 kHz, modulation amplitude 4 G, scan speed 0.2 MHz/s, 60 kHz broadening of RF excitation.

the heme of the hydroperoxo intermediate. The hyperfine coupling to a ^{14}N pyrrole ligand is close to isotropic and provides a good measure of the spin density on Fe. In addition, the principal values of the pyrrole ^{14}N quadrupole tensor are well known; 3**P** $\approx [-1.0, 3.2, -2.2]$, with the first value corresponding to the normal to the heme plane, the third corresponding to the Fe−N bond, and the second corresponding to the in-plane direction perpendicular to the plane of the first two.[28,29] Thus, determination of the orientation of 3**P** relative to the **g**-tensor frame discloses the orientation of **g** relative to the molecular axes, as shown earlier.[30] We used this technique to characterize the intermediates formed during the P450 reaction cycle.[7]

Figure 4 shows 35 GHz CW ^{14}N ENDOR spectra taken at g_1 for the hydroperoxoferri-HO intermediates, **P** and **R**. Previous work on a variety of low-spin hemoprotein derivatives and on model compounds suggested that the signal from the pyrrole nitrogens would be readily detected,[29,30] but that from the proximal ^{14}N histidyl ligand would not,[31−33] and in each spectrum there is a pair of doublets assigned as indicated to the $\nu_+(\pm)$ branches of two slightly distinguishable classes of pyrrole ^{14}N ligands (N1, N2);[34] we did not detect the histidyl ^{14}N. The

(28) Brown, T. G.; Hoffman, B. M. *Mol. Phys.* **1980**, *39*, 1073−1109.
(29) Scholes, C. P.; Lapidot, A.; Mascarenhas, R.; Inubushi, T.; Isaacson, R. A.; Feher, G. *J. Am. Chem. Soc.* **1982**, *104*, 2724−2735.
(30) Lee, H.-I.; Dexter, A. F.; Fann, Y.-C.; Lakner, F. J.; Hager, L. P.; Hoffman, B. M. *J. Am. Chem. Soc.* **1997**, *119*, 4059−4069.
(31) Mulks, C. F.; Scholes, C. P.; Dickinson, L. C.; Lapidot, A. *J. Am. Chem. Soc.* **1979**, *101*, 1645−1654.
(32) Scholes, C. P. In *Multiple Electron Resonance Spectroscopy*; Dorio, M. M., Freed, J. H., Eds.; Plenum Press: New York, 1979; pp 297−329.
(33) Scholes, C. P.; Falkowski, K. M.; Chen, S.; Bank, J. *J. Am. Chem. Soc.* **1986**, *108*, 1660−1671.
(34) We note that we cannot rule out an alternate pairing of the lines in each spectrum, although we do not favor it; it would give essentially identical (average) hyperfine couplings for the two types of nitrogens, while making their quadrupole couplings noticeably inequivalent.

more intense pair of features in the spectrum of **P** corresponds to pyrrole ^{14}N with $A1_1 = 5.11$ MHz, $|3P1_1| = 0.97$ MHz (eq 1a), and the less intense pair corresponds to $A2_1 = 5.53$ MHz, $|3P2_1| = 1.0$ MHz. An analogous assignment in the spectrum of **R** shows that the hyperfine and quadrupole couplings of N2 are the same, and those of N1 differ only slightly: $A1_1 = 4.98$ MHz, $|3P1_1| = 0.9$ MHz and $A2_1 = 5.5$ MHz, $|3P2_1| = 1.0$ MHz.

The similarity of the coupling constants for the **P** and **R** species confirms that these states are electronically the same, differing only in a slight structural relaxation. The values of the A_1 hyperfine couplings fall well within the range, $A_1 = 5.0-6.5$ MHz, found for low-spin ferri-Hb and -Mb derivatives, indicating that these intermediates appear as rather normal ferriheme states, with comparable spin density on the Fe(III) to that in the well-defined azido-Mb and -Hb complexes.[29] We obtained similar results for the heme ^{14}N ligands in the corresponding hyroperoxo (and peroxo) intermediates of cytochrome P450cam, which showed an average value at g_1 of $A_1 \approx 5.8-5.9$ MHz, with $|3P_1| \approx 0.9$ MHz.[7] As with spectra of the other ferriheme complexes taken at g_1, the observation for HO of such sharp peaks and small values of $3P_1$ in the single-crystal-like ENDOR spectra at g_1 indicates that g_1 lies essentially along the heme normal of **P** and **R**, as expected. Thus, it appears that neither the interactions that cause the large g_1 for the hydroperoxoferri-HO intermediates nor the difference in proximal ligands between HO (His) and P450 (Cys) alter the character of the ferriheme fragment of the enzyme-bound hydroperoxoferriheme.

Splitting of the Ferriheme "$(t_2)^5$" d-Orbital Manifold. To provide a heuristic electronic-structure correlate to the different *g*-values shown by the several reduced-dioxygen-ferriheme forms, we calculated the energies of the "t_2" orbitals of the d^5-ferric ion of these species from their *g*-values according to the well-known crystal-field model, which essentially ignores bonding effects in a direct way while reflecting them in the values of the splitting of the three t_2 orbitals.[35] The experimental determination by ^{14}N ENDOR spectroscopy that g_1 lies along the heme normal (see below) requires that the in-plane t_2 electron orbital (call it d_{xy}) lies below the two $d\pi$-t_2 orbitals (e.g., d_{xz}, d_{yz}), the higher energy of which contains the unpaired (fifth) electron of the d^5 ferric ion. The splitting of these two $d\pi$ orbitals ($\delta\epsilon_\pi$) reflects the degree of π bonding between Fe and O−O (out-of-plane with respect to the Fe−O−O plane). The calculations show that this splitting is larger for the H-bonded peroxoferriheme seen with the (D251N) mutant of P450cam ($g_1 = 2.25$ species; $\delta\epsilon_\pi/\lambda \approx 7.2$, where $\lambda = 460$ cm^{-1} is the spin−orbit coupling constant on Fe) than for the hydroperoxoferriheme of P450cam or β-Hb chains ($g_1 = 2.31$;[7] $\delta\epsilon_\pi/\lambda \approx 6$). This is as expected if Fe−O_2 π bonding is diminished by formation of the O−H bond at the distal O of the hydroperoxo anion. The splitting is further reduced in the **P** intermediate ($\delta\epsilon_\pi/\lambda \approx 5.2$), in support of the idea that the conformation of this species in HO reduces π bonding; the relaxation to **R** increases the splitting somewhat ($\delta\epsilon_\pi/\lambda \approx 5.8$), but it remains less than that of the g_1-2.31 species. Finally, in all of the species discussed, the overall splitting of the t_2 orbitals, the difference in energy between the highest and lowest t_2 orbital, remains roughly the same ($\delta\epsilon_{13}/\lambda \approx 9.5-11$).

(35) McGarvey, B. R. *Coord. Chem. Rev.* **1998**, *170*, 75−92.

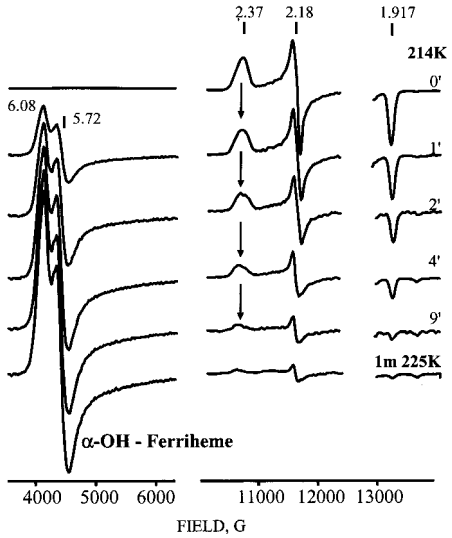

Figure 5. EPR spectra of cryoreduced oxy-HO after reaction at 214 K for indicated times and then at 225 K for 1 min. Conditions: as in Figure 1.

Reaction of Intermediate R To Form Ferri-α-hydroxoheme-HO Product (h). We showed before that the hydroperoxoferri-HO primary product, **P**, disappears upon annealing to 238 K, and this loss is accompanied by the appearance of the signal from the hydroxylation product, high-spin ferri-α-*meso*-hydroxyheme-HO (**h**), with $g_1 = 6.07$ and $g_2 = 5.72$.[8] We now demonstrate that **R** is the kinetically competent reactant in this conversion.

The time course of the loss of **R** during the **R** → **h** conversion at 214 K could be experimentally followed through successive annealing steps at this temperature by collecting EPR spectra at 2 K after 1, 2, 4, and 9 min of annealing at 214 K, taking as the "zero-time" **R** spectrum the one collected after the annealing step at ∼200 K; to follow the formation of **h**, we subtracted the signal of the residual aquoferri-HO as found in the spectrum taken after annealing at ∼200 K. Figure 5 presents these data. As can be seen, the **R** signal decreases with progressive annealing at 214 K. However, the process is not simple in that one can see that by 4′ annealing at 214 K the shape of the g_1 feature has begun to change, with the maximum intensity shifting slightly to lower field; by 9′ the g_1 feature is at $g_1 = 2.39$. We interpret this to mean that the reaction being followed involves **R** and that the **R1** minority conformation reacts more slowly, or does not react at all, at this annealing temperature. ^{14}N ENDOR spectra of **R/R1** taken at the stages of reaction 214 K (not shown) show a loss in ^{14}N signal intensity that parallels the loss of EPR signal. In addition, the resolution of the^{14}N peaks decreases, in part perhaps because of the poorer S/N, but likely in most part because the less reactive **R1** that persists near the end of the reaction is slightly heterogeneous and displays a small dispersion in A_1 and/or P_1 values.

In parallel with this reaction of **R**, the signal of ferri-α-*meso*-hydroxyheme-HO (**h**; $g_1 = 6.07$ and $g_2 = 5.72$)[26] appears and grows during the 214 K annealing process, Figure 5. The procedure of quantifying **h** by simply subtracting the zero-time high-spin aquoferri-HO spectrum assumes that there is no autoxidation to the ferriheme-HO resting state during this reaction process, and this is confirmed by the observation that the signal from **h** in the g-6 region grows without appreciable change in shape. Interestingly, the fact that the *g*-values of **h**

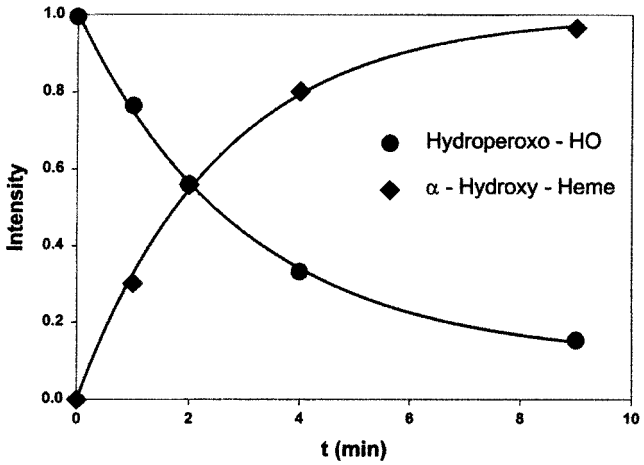

Figure 6. Kinetics of the catalytic conversion at 214 K from hydroperoxoferri-HO, **R** (●), to ferri-α-*meso*-hydroxyheme, **h** (◆). Intensities of EPR signals from **R** and **h** were obtained from Figure 4 as described in text. The relative intensities for **R** were obtained by normalizing to the zero-time spectrum; those for **h** were obtained by normalizing to the $t \rightarrow \infty$ intensity provided by the fit to an exponential rise. The solid lines are the results of a fit to an exponential fall of **R** ($I \propto a + b(\exp(-t/\tau))$, $\tau =$ 3 min, $a = 0.1$, $b = 0.9$ (see text), and an exponential rise for **h**, $\tau = 2.5$ min.

formed at 214 K are those of the thermally equilibrated, five-coordinate α-*meso*-hydroxyheme-HO[26] means that the water molecule formed during the reaction (Scheme 1) is released by Fe at this temperature.

To analyze the kinetics of reaction at 214 K, we measured the heights of the absorption-like g_1 feature in the reactant **R/R1** derivative spectrum and the peak-trough heights of the g-6 signal of product **h** in Figure 5, and we plotted the signal intensities versus annealing time in Figure 6. The excellent fit to an exponential rise with rise time (1/*e* time) of $\tau = 2.5$ min is overlaid on the plot of the **h** intensities; the fit to an exponential decay ($I \propto a + b(\exp(-t/\tau)$; $a + b = 1$) with $\tau = 3$ min is overlaid on the plot of the relative intensities of the $g_1 = 2.38$ feature of **R/R1**. Thus, the hydroxylation product **h** forms synchronously with the loss of the hydroperoxoferri-HO intermediate, **R**.

The function employed to describe the exponential decay attributes a fractional intensity (*b*) to form **R**, while allowing for a fraction of the intensity (*a*) that does not decay. The latter represents the contribution of **R1**, which is unreactive or slowly reactive at this temperature. The fit gives a fraction $a = 0.1$ for this persistent signal at the field chosen for measurement. While qualitative examination of the overall contributions of the two forms suggests this fraction is not unreasonable for the total contribution of **R1** to the EPR spectrum, precise quantitation of the two forms is not possible.

Annealing at 225 K and Above. A further annealing step at 225 K appreciably decreases the small remaining **R1** signal (Figure 5), and it disappears completely after a step at 240 K (not shown). These two steps are accompanied by increases in the high-spin signal around g-6 that likely include contributions from nonenzymatic autoxidation of the oxy-HO that had not been cryoreduced; this is seen during annealing of other cryoreduced oxyhemoproteins.[7,13] Hence, it is not possible to say whether the residual **R1** seen in the 225 and 240 K spectra is competent to produce **h** at temperatures greater than 214 K.

Annealing to 273 K caused an increase in the high-spin signal, presumably from autoxidation of oxy-HO. When the sample

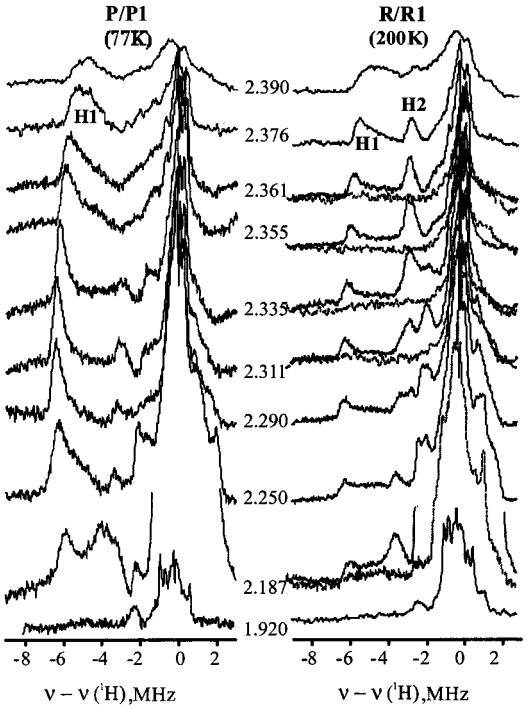

Figure 7. Orientation-selective, 2-D field/frequency ^{1}H CW ENDOR patterns for cryoreduced oxy-BHO intermediate **P** (77 K) and for the intermediate **R/R1** annealed at 200 K for 1 min (200 K). Solid line, H_2O buffer; dashed line, D_2O buffer. Conditions: $T = 2$ K, field modulation 100 kHz, modulation amplitude ~1 G, scan speed 0.5 MHz/s, 30 scans, 60 kHz broadening of RF excitation, MW frequency 35.263 Ghz.

was then rewarmed to room temperature and flushed with O_2, the hydroxy-heme product **h** reacted further, and its signal disappeared.

^{1}H ENDOR Studies of P and R/R1 Intermediates. We employed 35 GHz ^{1}H ENDOR spectroscopy to further characterize the changes in the hydroperoxoferri-HO heme pocket that occur upon the annealing/relaxation conversion from **P** to **R/R1** and to explore the features that make **R** catalytically reactive, but **R1** less so, or not. A ^{1}H signal is a doublet, symmetric in frequency about ν_H according to eq 1; a commonly occurring asymmetry in intensities renders the υ_+ branch not only redundant according to eq 1, but less useful for measurements. We present only the ν_- branch of each spectrum and plot frequencies as $\delta\nu = \nu - \nu_H$; thus $\delta\nu$ for a ν_- signal is negative. To discuss the ν_- features we often note the magnitude of $\delta\nu$ as the frequency offset.

We collected 2-D, field/frequency datasets comprised of ENDOR spectra collected at numerous points across the EPR envelopes of **P** and **R/R1** prepared in H_2O and D_2O buffers; selected spectra are shown in Figure 7. As reflected in the figure, these experiments were constrained by an inability to collect spectra in a field range around $g = 2$, where there are strong EPR signals from free radicals created by the irradiation; this corresponds to most of the field range between roughly g_2 and g_3 of the cryoreduced oxyheme centers. As illustrated by the several spectra shown for samples prepared in D_2O buffers, all the ^{1}H signals with $A \gtrsim 3.5$ MHz (offset $\gtrsim 1.7$ MHz) are exchangeable in both **P/P1** and **R/R1**.

Like hydroperoxoferri-Mb,[16] -Hb,[8] and P450cam,[7] both the **P** (Figure 7, left) and **R/R1** (Figure 7, right) forms of hydroperoxoferri-HO[8] give an ENDOR signal at the low-field

(g_1) edge of the EPR spectrum from an exchangeable proton, denoted H1, which has a substantial hyperfine coupling ($A(g_1) \approx 10-11$ MHz in Figure 7) and which is assigned to the proton of the hydroperoxo moiety. In addition, both g_1 spectra show an intense, poorly resolved ^{1}H signal that is centered at the proton Larmor frequency and is of ~4−5 MHz in breadth. As shown in the figure, this signal includes intensity both from exchangeable and from nonexchangeable protons.

Considering the 2-D pattern for **P/P1**, Figure 7, left, one sees that the ν_- peak for H1 in the g_1 spectrum of **P** broadens and spreads as the field is increased (g decreased). There is a well-defined outer branch whose offset smoothly increases to a maximum value, corresponding to a maximum coupling of A_{max}(H1) = 12.9(2) MHz, at $g = 2.29$, then decreases (decreasing A) as the field is further increased through g_2 to $g \approx 2.1$, beyond which the free-radical signals preclude further examination until the g_3 region. Spectra taken near g_3 again show a single ν_- peak where A_3(H1) ≈ 5 MHz. The shift of the outer ν_- branch to greater offset (higher A) as g increases from g_1 is accompanied by a growth of intensity with lower offset (lower A), which forms a poorly defined inner ν_- branch. This branch quickly merges with intensity from other exchangeable protons with smaller couplings.

The maximum hyperfine coupling of A_{max}(H1) = 12.9(2) MHz corresponds to the maximum component of the H1 hyperfine tensor. This value is less than that seen for a H-bonded peroxoferri-P450, A_{max} =14.4, but greater than that for hydroperoxoferri-P450, A_{max} = 11.2 MHz,[7] again highlighting the unusual characteristics of hydroperoxoferri-HO, **P**. The occurrence of the maximum hyperfine coupling at a field away from a principle g-value requires that the hyperfine tensor be noncoaxial with the **g**-tensor. On the assumption that the H1 hyperfine tensors for **P** and hydroperoxoferri-P450cam behave similarly, the appearance of the maximum coupling at $g \approx 2.29$ for **P** indicates that this tensor direction makes a polar angle, $\theta \approx 40°$, with the g_1 direction, which was shown above to be perpendicular to the heme plane. However, the poor definition of the inner ν_- branch and the presence of signals from other, more weakly coupled protons make a detailed tensor analysis unfeasible.

The 2-D ENDOR pattern for **R/R1**, Figure 7, right, contains an H1 pattern whose outer edge in particular behaves very similarly to that of **P**. Following the outer edge of the ν_- branch for H1, the hyperfine coupling increases with field to a (slightly smaller) maximum value, A_{max} = 12 MHz at g-2.29, then decreases with a further increase in field (decrease in g); likewise, spectra collected at the extreme low-field edge of the EPR spectra of **P** and **R/R1** are not significantly different.

However, the full 2-D ENDOR pattern shows a dramatic difference at smaller frequency offset; as the magnetic field is raised only slightly into the g_1-feature of **R/R1**, one sees the sudden appearance of a sharp, intense ν_- peak from a second exchangeable proton, denoted H2, at $\delta\nu \approx -2.7$ MHz (A = 5.4 MHz). The H2 signal persists throughout the remainder of the **R/R1** spectra, appearing to split as the observing g-value decreases beyond $g \approx 2.27$.[36] Noting that the EPR spectrum is a superposition of the spectra from the majority species (**R**) and the minority species (**R1**), and that the latter has a slightly larger value of g_1 and thus dominates the EPR intensity at the extreme low-field edge of the EPR envelope, we interpret the 2-D ENDOR pattern to mean that annealing at temperatures below 200 K allows a reorganization in the distal-pocket H-bond network so as to create a structurally well-defined, hyperfine-coupled, H2 site.

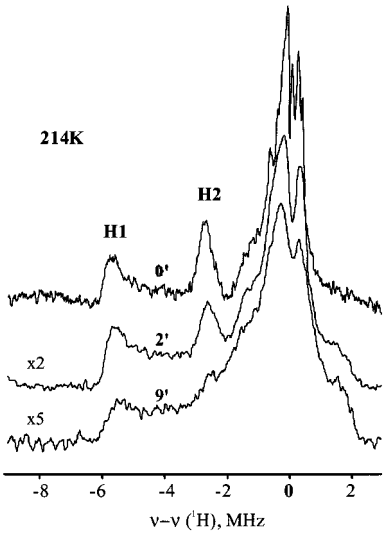

Figure 8. ^{1}H CW ENDOR spectra taken at g_1 = 2.366 for cryoreduced oxy-HO reacted at 214 K for 0, 2, and 9 min, respectively. Conditions: as in Figure 7.

That H2 is associated only with the reactive substate **R** is confirmed when one examines normalized ^{1}H ENDOR spectra collected at 214 K during the **R** → **h** catalytic conversion, Figure 8 (g = 2.366). The total (absolute) intensity of the spectrum decreases in parallel with the loss of the EPR signal from **R**, as indicated by the normalization factors listed in the figure. As a result of the normalization, it seems that the H2 peak from **R** disappears while that of H1 remains. However, when one takes into account the overall decrease in intensity, the figure instead shows that both H1 and H2 signals are associated with the reactive majority species, **R**, and that these are lost together during the reaction, while the nonreactive (or more slowly reacting) minority species, **R1**, has a spectrum that exhibits only an H1 signal.

The simplest interpretation of this result is that H2 represents a newly formed H-bond to the hydroperoxo moiety, whose proton is H1. However, despite a concern not to overinterpret CW ENDOR intensities, it is clear that the H1 signal from **R** is appreciably weaker relative to the signal near to the proton Larmor frequency than is the case for **P/P1**. This opens the possibility that H2 is not a second proton. Instead, it might be that **R** represents two conformers of the hydroperoxoferriheme, one with H1 as the associated proton and the other with H2.[37] Future experiments will address this issue.

Cryoreduction of Oxy-HO (D140X). To probe the "microscopic" consequences of the D140X mutations, which create major changes in catalytic function,[17,18] we prepared oxy-HO (D140X), X = A, F, and subjected them to 77 K cryoreduction and subsequent annealing. The EPR spectra of the resting-state ferri-HO (D140X) have not been described. WT-ferri-HO gives a homogeneous high-spin ferriheme signal with $g_z \approx 5.75$,[26]

(36) The limited ability to track the full spectrum of H2 over a large field range precludes the determination of its hyperfine tensor.

(37) We thank a perceptive reviewer for encouraging us to note the two alternatives.

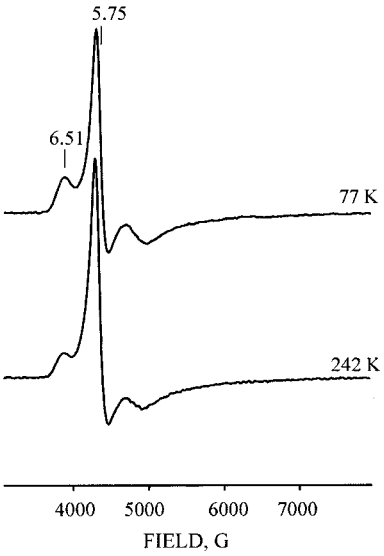

Figure 9. g-6 region of Q-band EPR spectra of 77 K cryoreduced oxy-HO D140A mutant HO and after annealing to 242 K in steps, as discussed in text. Conditions: as in Figure 2 except 35.163 Ghz.

while the D140A mutant gives a heterogeneous signal with one form whose signal is similar to that of WT enzyme and a second that seems to have a rhombic signal with $g_1 = 6.5$ and $g_2 \approx 5.3$, as seen in the residual high-spin signal obtained from cryoreduced oxy-HO (D140A), Figure 9,[38] while the EPR spectrum of ferri-D140F is homogeneous and similar to that of the WT enzyme (not shown).

Figure 10 presents the spectrum of the low-spin ferriheme species produced by 77 K cryoreduction of oxy-HO (D140A). It is qualitatively similar to that of the H-bonded-peroxoferri state of Mb and Hb[11−14] and of the P450cam (D251N) mutant,[7] with $g_1 \approx 2.25$. However, the product is not homogeneous; at least two components can be discerned, the second having $g_1 \approx 2.23$, and there are two g_2 features, at 2.174 and 2.141. An analogous result is seen for cryoreduced oxy-HO (D140F) (not shown). We interpret this to mean that the distal pocket in both the mutant enzymes is disordered, as suggested by the ferri-HO (D140A) EPR spectrum; further, the mutations have interrupted the delivery of proton H1 at 77 K, so that the peroxoferriheme-HO rather than hydroperoxoferriheme forms at this temperature.[39]

Upon annealing the D140A sample to 181 K for 1″, the signal converts to one with a majority species which has $g_1 \approx 2.36$ and $g_2 \approx 2.18$, although it remains heterogeneous. This conversion indicates that the H1 proton is delivered to a large fraction of the ensemble of cryoreduced oxy-HO and that these adopt the unusual structure characteristic of the HO distal pocket. With further annealing to 189 K (not shown) and then 200 K, Figure 10, the hydroperoxoferri species relaxes to a well-defined state, denoted **R′(140A)**, with $\mathbf{g} = [2.36, 2.18, 1.915]$; one can also see a broad feature between g_1 and g_2, which is the g_2 feature from a small amount of low-spin ferri-HO (D140A). Surprisingly, the **R′(140A)** signal changes little upon annealing to 210 K for 2.5″, 220 K for 1″, and then 228 K for 1″, by

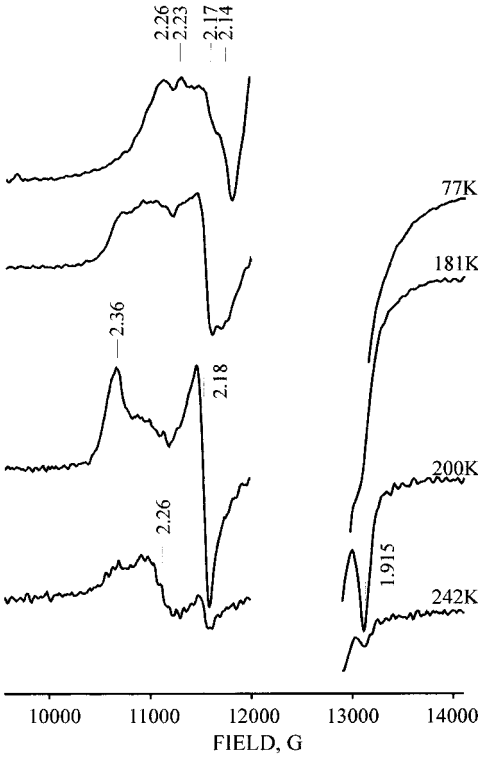

Figure 10. Low-spin ferriheme Q-band EPR spectra of oxy-HO (D140A) radiolytically reduced at 77 K and annealed at the indicated temperatures for 1 min. Free radicals signals around $g = 2$ are omitted for clarity. Conditions: as in Figure 2 except 35.163 Ghz.

which temperature the hydroperoxoferri-HO-WT would have reacted to form product. Upon further warming to 242 K for 1″, this signal is almost completely lost, revealing the underlying signal from low-spin ferri-HO, in parallel. In this process there is little increase in the intensity of the high-spin ferri-HO (D140A) signal and no evidence for the buildup of the rhombic high-spin signal from the α-hydroxo-heme product, Figure 9. Thus, the **R′(140A)** species does not convert to an EPR-active form, and it does not form product.

The EPR spectrum of 77 K cryoreduced oxy-HO (D140F) is weaker, but otherwise similar to that of the D140A mutant in that it produces a broadened g_1-2.25 species (not shown). Annealing to 181 K likewise creates a heterogeneous hydroperoxoferri-HO spectrum, $g_1 \approx 2.34$, somewhat less than the characteristic $g_1 = 2.37$ value; annealing to 205 K causes a sharpening of the signal, but g_1 remains low, $g_1 = 2.34$. Thus, the heme pocket in the D140F mutant appears to be not only so disorganized as to abolish catalysis, but even to alter the characteristics of the hydroperoxoferri-HO.

Proton ENDOR spectra of the 77 K-cryoreduced oxy-HO (D140A) g_1-2.25 species show a signal from an exchangeable proton with coupling of $A \approx 14$ MHz at g_1, consistent with the behavior of other H-bonded peroxoferriheme proteins, but the spectrum differs in being very poorly resolved (Figure 11), consistent with the picture of a disordered heme pocket. The $g_1 = 2.37$ proton ENDOR spectrum of hydroperoxoferri-HO (D140A) formed by annealing to 200 K shows the signal from the H1 proton, with $A(g_1) \approx 11$ MHz, as expected, and also shows the H2 signal with $A(g_1) \approx 5$ MHz. However, comparison with the ^{1}H ENDOR spectra of the reactive species **R** (Figure 7) shows that the H1 and H2 features for **R′(140A)** are

(38) One cannot rule out that the minority species is instead axial, but very broad.

(39) We note that the signal trails sufficiently to low field that it appears that a small percentage of the signal has $g1 \approx 2.3$, characteristic of a typical hydroperoxoferriheme species. However, that more likely reflects a trace of low-spin ferri-HO, to be discussed presently.

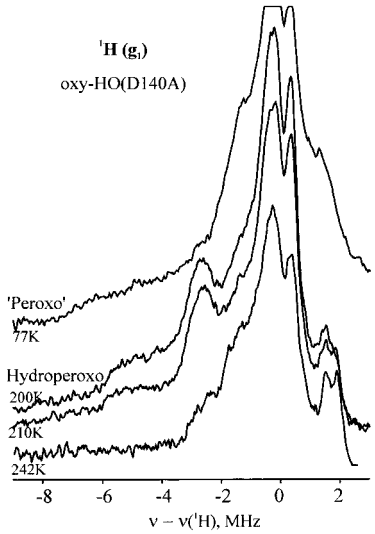

Figure 11. ^{1}H CW ENDOR spectra taken at the g_1 field for cryoreduced oxy-HO (D140A) primary reduction product, $g_1 = 2.26$; after annealing at 200, 228, and 242 K for 1 min, $g_1 = 2.36$. Conditions: as in Figure 7 except 35.163 GHz.

noticeably broader, indicative of distal-pocket disorder. The **R′(140A)** proton ENDOR spectrum, like its EPR spectrum, is not altered by annealing to 210 K for 2.5″. The EPR spectrum of cryoreduced oxy-HO (D140F) was too weak to permit ENDOR characterization.

Discussion

The present cryoreduction EPR/ENDOR experiments have allowed a detailed examination of the reactive intermediates involved in the activation of dioxygen by HO and the catalytic conversion of heme to α-*meso*-hydroxyheme. In the process, we have characterized the kinetically competent reactant in this conversion, hydroperoxoferri-HO (**R**), and obtained information about the microscopic basis of the striking effects on reactivity produced by mutation at position D140.[17,18] The resulting reaction cycle is summarized in Scheme 2.

One-electron cryoreduction of oxy-ferrous HO at 77 K yields a hydroperoxoferri-HO species, denoted **P**.[40] This formation of a hydroperoxo-HO species at 77 K clearly indicates that the O_2 moiety of the precursor oxy-HO is stabilized by an H-bond poised to deliver its proton upon electron injection, with the proton in this H-bond becoming the hydroperoxo-proton H1, the first proton delivered to reduced dioxygen during catalysis. Such a hydrogen-bonding interaction with the bound O_2 had been inferred previously from EPR studies on cosubstituted HO.[41] It is compatible with the crystal structure reported for ferric HO,[17,18,42] which suggests that a water network anchored by the carboxyl group of D140 and the carbonyl oxygen of T135 could H-bond to and stabilize the heme-bound dioxygen in a structure that is optimal for reduction and prompt proton transfer. It is important to note that a hydroperoxoferri species also forms upon 77 K cryoreduction of the other oxygen-activating enzymes

Scheme 2

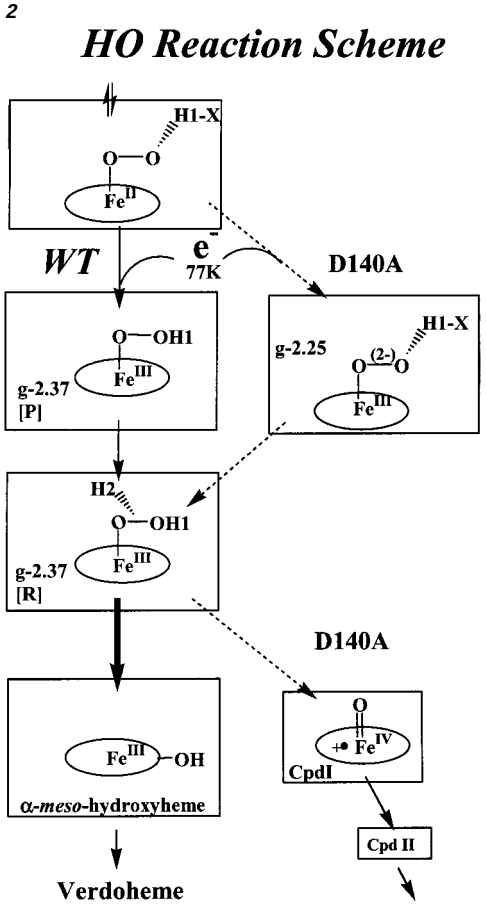

we have studied, oxy-P450cam,[7] whereas 77 K cryoreduction of the oxygen-transporting proteins, MbO_2 and HbO_2, instead yields an H-bonded peroxoferri species, with proton transfer to form the hydroperoxoferri species occurring only at temperatures above ∼180 K.[11,13] This supports the idea that the distal pockets of the O_2 complexes of the dioxygen-activating enzymes HO and P450cam contain a hydrogen-bonding network designed for efficient transfer of the first proton of catalysis and that such a system distinguishes these enzymes from the oxygen-carrying proteins. It seems likely that proton delivery to the reduced dioxygen involves an $R-COOH-(H_2O)_n-\{[O_2^{2-}]-Fe^{3+}\}$ motif, where the carboxyl group comes from Asp251 in P450cam,[43] and D140 in HO,[42] based on the finding that mutation to these residues hinders delivery of the first proton to form the hydroperoxo moiety in both enzymes.[7]

The immediate product of 77 K cryoreduction of oxy-HO (form **P**) is constrained to retain a conformation close to the equilibrium conformation of the precursor, HO-O_2. As a rule, this would be a nonequilibrium conformation for the product of cryoreduction, which typically relaxes to an equilibrium state at higher temperatures. Upon annealing the cryoreduced HO to 200 K, we in fact see that a rearrangement of the distal pocket, presumably including the putative water network and possibly the protein side chains, generates a majority hydroperoxo-form, **R**, plus a minority form **R1**. The intermediates **P** and **R** both are "normal" ferriheme species as shown by their ^{14}N ENDOR spectra and are confirmed as hydroperoxoferri-HO forms by

(40) The EPR spectra of cryoreduced oxycomplexes of HO and the mutants exhibit signals from minor species reflecting the presence in solution of a few structurally distinct subpopulations of oxy-HO. We ignore them unless they have significance in understanding function.
(41) Fujii, H.; Dou, Y.; Zhou, H.; Yoshida, T.; Ikeda-Saito, M. *J. Am. Chem. Soc.* **1998**, *120*, 8251−8252.
(42) Schuller, D. J.; Wilks, A.; Ortiz De Montellano, P. R.; Poulos, T. L. *Nat. Struct. Biol.* **1999**, *6*, 860−867.
(43) Hishiki, T.; Shimada, H.; Nagano, S.; Egawa, T.; Kanamori, Y.; Makino, R.; Park, S.-Y.; Adachi, S.-I.; Shiro, Y.; Ishimura, Y. *J. Biochem. (Tokyo)* **2000**, *128*, 965−974.

the observation of an ^{17}O hyperfine coupling to the proximal hydroperoxo-oxygen that is the same as that of hydroperoxo-β-Hb chains. However, the EPR spectrum of hydroperoxoferri-HO shows a large value, $g_1 = 2.37$, as compared to that of other hydroperoxoferriheme species with $g_1 \approx 2.3$. Further, the ^1H ENDOR spectra of the hydroperoxo proton (H1) show a slightly larger maximum hyperfine coupling than for the hydroperoxoferrihemes of Hb, Mb, and P450cam, and the d$-\pi$ splittings of the t_2 orbitals on the ferric ion of the HO species are relatively low. We propose that these characteristics reflect an unusually acute Fe$-$O$-$O angle in oxy- and hydroperoxo-HO that is forced by the HO distal-pocket environment, as suggested previously from resonance Raman studies of oxy-HO[44] and from EPR studies of O_2-Co$-$HO.[41] The analysis of t_{2g} orbital energies further supports the idea that distal-pocket constraints orient the [OOH] moiety toward the α-*meso* carbon of the heme, as this would tend to minimize the d-orbital splitting on Fe. In short, the EPR characteristics of **P** and **R** suggest that the distal pocket of HO is so organized as to direct the terminal hydroperoxo "OH" toward the site of reaction.

After the rearrangement to form the hydroperoxoferri-HO intermediate **R**, the enzyme is prepared for the actual hydroxylation step: **R** reacts at 214 K, and its disappearance is accompanied by the synchronous formation of the α-*meso*-hydroxyheme product, **h**. The agreement between the decay time of **R** and the rise time of **h**, with $\tau \approx 2-3$ min at 214 K, establishes that **R** is the kinetically competent intermediate that reacts in the rate-limiting step which generates **h**.

R, Actual Hydroxylating Intermediate. The observation that **R** is kinetically competent does not, of course, require that **R** converts directly to **h**. It admits the possibility that the rate-limiting step involves heterolytic cleavage of the O$-$O bond to form a reactive high-valence, compound I-like species, followed by its rapid conversion of the compound I-like heme to **h**. However, this possibility is ruled out by the results for the HO (D140X) mutants.

The importance of the Asp140 in the WT H-bond network in the distal pocket has been shown recently by reports of the effects on HO activity of mutating this residue.[17,18] Mutation of Asp140 to nonpolar Ala or Phe destabilizes oxy-HO, reduces (Ala) or abolishes (Phe) heme oxygenase activity, and increases peroxidase activity. The present study gives microscopic insights into the influence of this mutation and has allowed us to confirm that **R** converts directly to **h**.

Regarding the first proton of catalysis, 77 K cryoreduction of the oxy complexes of the D140A and D140F mutants yields an H-bonded peroxo-HO, as with croyreduced oxy-Mb and -Hb, not the hydroperoxoferri-HO formed by cryoreduction of the WT oxy-HO. Presumably, mutation of Asp140 to nonpolar Ala and Phe disturbs the H-bonding network so as to impede proton transfer to the peroxo ligand directly formed by cryoreduction at 77 K. In these mutants, the proton transfer occurs only after annealing to $T > 180$ K, being facilitated by rearrangements of the distal pocket that are encouraged by the negative charge of the peroxo ligand and allowed by the increased mobility at higher temperatures.

The hydroperoxoferri-HO (D140F) has an EPR spectrum, and thus a structure, that is different from that of the active hydroperoxo-HO intermediate **R**; it is less stable than **R** and does not react to form α-*meso*-hydroxoheme. The latter is in agreement with the reported absence of heme oxygenase activity of this mutant at room temperature.[17,18] In contrast, the hydroperoxoferri-HO (D140A) intermediate denoted **R′(140A)** shows EPR and ^1H ENDOR spectra very similar, although not identical, to those of the active WT intermediate **R**. In particular, the ^1H ENDOR signals of the H1 and H2 protons of **R′(140A)** are broadened, indicating a disorder in the environment of its hydroperoxo moiety.

Despite its overall similarities to the WT species **R**, intermediate **R′(140A)** only reacts at the higher temperature of 240 K, and this is not accompanied by the formation of the high-spin-ferric α-*meso*-hydroxoheme product. In fact, this reaction of **R′(140A)** is accompanied by only a minimal increase of the high-spin EPR signal of ferri-HO (D140A), Figure 9, and it is likely that this small increase is in large part due to autoxidation of oxy-HO, as seen for other oxyhemoproteins (MbO_2, HbO_2, and P450cam-O_2). As there is no reductant present in the annealed cryoreduced sample that could reduce the ferriheme of **R′(140A)** to the EPR-silent ferrous form, we infer that intermediate **R′(140A)** converts essentially quantitatively to an EPR-silent compound II-like state at 240 K, presumably through formation and rapid reduction of a compound I-like species, Scheme 2; such a process has been shown to occur in the reaction of the mutant HO with H_2O_2.[17,18]

The suggestion that the hydroperoxoferri-HO (D140A) converts to a "noncompetent" ferryl form is consistent with the reported experimental data on the catalytic activity of this mutant.[17,18] Unlike HO (WT), the D140A and F HO mutants were reported to show peroxidase activity but reduced oxygenase activity in reaction with H_2O_2. They instead form an unreactive compound II-like intermediate upon reaction with H_2O_2,[17,18] although the formation of compound II has not been recorded during a reaction with O_2 and reductase. As shown by Fujii et al.,[18] in the presence of NADPH-cytochrome P450 reductase, the D140A mutant converted 50% of the bound heme to the verdoheme$-$CO complex while consuming 3.5 equiv of NADPH. This corresponds to the formation of $\sim$0.2 equiv of verdoheme$-$CO per equivalent of NADPH consumed. Such a low yield of the reaction also may be explained by formation of an enzymatically inactive ferryl (compound II) form. It may be that this intermediate is not detected in the reaction with NADPH-cytochrome P450 reductase because it is reduced efficiently by the reductase.

Most importantly, the conclusion that the ferri-hydroperoxo species in the D140A mutant forms a high-valence intermediate, and that it is not catalytically active, shows that the kinetically competent reactive hydroperoxoferri species **R** of the WT enzyme does not generate compound I as a catalytically active, but undetected, intermediate on the reaction pathway to product, but rather that **R** indeed reacts directly to form product.

We thus conclude that the rate-limiting step for **R** $\rightarrow$ **h** conversion is the actual attack of the hydroperoxo moiety on the meso α-carbon. This conclusion for hydroxylation through activation of O_2 conforms to the earlier conclusion by Ortiz de Montellano and co-workers based on experiments with peroxides.[2] Proton ENDOR shows that the active hydroperoxo intermediate **R** exhibits a second well-defined ^1H signal, denoted H2, which is introduced by annealing to 200 K, but is not seen

(44) Takahashi, S.; Ishikawa, K.; Takeuchi, N.; Ikeda-Saito, M.; Yoshida, T.; Rousseau, D. L. *J. Am. Chem. Soc.* **1995**, *117*, 6002$-$6006.

in the unreactive minority intermediate form, **R1**. Proton H2 may be part of a hydrogen bond that activates the O−O bond for cleavage, or it may represent a second, perhaps activated, conformation of the hydroperoxo moiety. The direct attack of the remote hydroperoxo oxygen on the heme α-carbon is presumably followed by rearrangement and proton "back-transfer" from the putative tetrahedral intermediate to yield the aquoferri-α-*meso*-hydroxyheme, which loses water at 214 K to form the five-coordinate equilibrium form of **h**.[2]

Summary

The present results show that the first monooxygenation reaction of HO and its D140 mutants follows Scheme 2. (i) The HO distal-pocket hydrogen-bonding network controls the geometry of the oxy ferrous heme through an H-bond network that (ii) delivers the first proton of catalysis to form the hydroperoxo moiety promptly upon electron injection even at 77 K and (iii) controls the geometry of this moiety for the hydroxylation step. (iv) Thermal rearrangement of the distal pocket after the dioxygen reduction and H1 proton-transfer steps is enabled by annealing to ∼200 K. With the catalytically competent distal heme-pocket structure of native HO thus having created the proper enzymatically reactive form of the hydroperoxoferri state (**R**), then (v) the remote O of the hydroperoxy moiety of **R** directly attacks the heme α-carbon in the step that forms the hydroxylated heme product, **h**. The D140A mutation (vi) diverts the hydroperoxoferri-HO from its catalytic reaction and appears to lead to the accumulation of a nonreactive compound II.

Acknowledgment. This work has been supported by the NIH (HL13531, GM57272) and by Grants in Aid from the Ministry of Education, Science, Sport, and Culture, Japan (12147201, 1248016, 12640549, 12680625).

JA0122391